OXFORD

Alignment of dynamic networks

V. Vijayan[1], D. Critchlow[1,2] and T. Milenković[1,*]

[1]Department of Computer Science and Engineering, ECK Institute for Global Health, and Interdisciplinary Center for Network Science and Applications (iCeNSA), University of Notre Dame, Notre Dame, IN 46556, USA and [2]Department of Physics and Astronomy, Austin Peay State University, Clarksville, Tennessee, TN 37044, USA

*To whom correspondence should be addressed.

Abstract

Motivation: Network alignment (NA) aims to find a node mapping that conserves similar regions between compared networks. NA is applicable to many fields, including computational biology, where NA can guide the transfer of biological knowledge from well- to poorly-studied species across aligned network regions. Existing NA methods can only align static networks. However, most complex real-world systems evolve over time and should thus be modeled as dynamic networks. We hypothesize that aligning dynamic network representations of evolving systems will produce superior alignments compared to aligning the systems' static network representations, as is currently done.

Results: For this purpose, we introduce the first ever dynamic NA method, DynaMAGNA++. This proof-of-concept dynamic NA method is an extension of a state-of-the-art static NA method, MAGNA++. Even though both MAGNA++ and DynaMAGNA++ optimize edge as well as node conservation across the aligned networks, MAGNA++ conserves static edges and similarity between static node neighborhoods, while DynaMAGNA++ conserves dynamic edges (events) and similarity between evolving node neighborhoods. For this purpose, we introduce the first ever measure of dynamic edge conservation and rely on our recent measure of dynamic node conservation. Importantly, the two dynamic conservation measures can be optimized with any state-of-the-art NA method and not just MAGNA++. We confirm our hypothesis that dynamic NA is superior to static NA, on synthetic and real-world networks, in computational biology and social domains. DynaMAGNA++ is parallelized and has a user-friendly graphical interface.

Availability and implementation: http://nd.edu/~cone/DynaMAGNA++/.

Contact: tmilenko@nd.edu

Supplementary information: Supplementary data are available at *Bioinformatics* online.

1 Introduction

Networks can be used to model complex real-world systems in a variety of domains (Boccaletti *et al.*, 2006). Network alignment (NA) compares networks with the goal of finding a node mapping that conserves topologically or functionally similar regions between the networks. NA has been used in many domains and applications (Emmert-Streib *et al.*, 2016). In computer vision, it has been used to find correspondences between sets of visual features (Duchenne *et al.*, 2011). In online social networks, NA has been used to match identities of people who have different account types (e.g. Twitter and Facebook) (Zhang *et al.*, 2015). In ontology matching, NA has been used to match concepts across ontological networks (Bayati *et al.*, 2013). Computational biology is no exception. In this domain, NA has been used to predict protein function (including the role of proteins in aging), by aligning protein interaction networks (PINs) of different species, and by transferring functional knowledge from

a well-studied species to a poorly-studied species between the species' conserved (aligned) PIN regions (Elmsallati *et al.*, 2016; Faisal *et al.*, 2015a,b; Guzzi and Milenković, 2017; Meng *et al.*, 2016b). Also, NA has been used to construct phylogenetic trees of species based on similarities of their PINs or metabolic networks (Kuchaiev *et al.*, 2010; Kuchaiev and Pržulj, 2011).

NA methods can be categorized as local or global (Guzzi and Milenković, 2017; Meng *et al.*, 2016b). Local NA typically finds *highly conserved* but consequently *small* regions among compared networks, and it results in a *many-to-many* node mapping. On the other hand, global NA typically finds a *one-to-one* node mapping between compared networks that results in *large* but consequently *suboptimally conserved* network regions. Clearly, each of local NA and global NA has its (dis)advantages (Guzzi and Milenković, 2017; Meng *et al.*, 2016a,b). In this paper, we focus on global NA, but our ideas are applicable to local NA as well. Also, NA methods can be

categorized as pairwise or multiple (Faisal *et al.*, 2015b; Guzzi and Milenković, 2017; Vijayan and Milenković, 2016). Pairwise NA aligns two networks while multiple NA can align more than two networks at once. While multiple NA can capture conserved network regions between more networks than pairwise NA, which may lead to deeper biological insights compared to pairwise NA, multiple NA is computationally much harder than pairwise NA since the complexity of the NA problem typically increases exponentially with the number of networks. This is why in this paper we focus on pairwise NA, but our ideas can be extended to multiple NA as well. Henceforth, we refer to global and pairwise NA simply as NA.

Existing NA methods can only align static networks. This is because in many domains and applications, static network representations are often used to model complex real-world systems, independent of whether the systems are static or dynamic. However, most real-world systems are dynamic, as they evolve over time. Static networks cannot fully capture the temporal aspect of evolving systems. Instead, such systems can be better modeled as dynamic networks (Holme, 2015). For example, a complex system such as a social network evolves over time as friendships are made and lost. Static networks cannot model the changes in interactions between nodes over time, while dynamic networks can capture the times during which the friendships begin and end. Other examples of systems that can be more accurately represented as dynamic networks include communication systems, human or animal proximity interactions, ecological systems, and many systems in biology that evolve over time, including brain or cellular functioning. In particular, regarding the latter, while cellular functioning is dynamic, current computational methods (including all existing NA methods) for analyzing *systems-level* molecular networks, such as PINs, deal with the networks' static representations. This is in part due to unavailability of experimental dynamic molecular network data, owing to limitations of biotechnologies for data collection. Yet, as more dynamic molecular (and other real-world) network data are becoming available, there is a growing need for computational methods that are capable of analyzing dynamic networks (Przytycka and Kim, 2010; Przytycka *et al.*, 2010), including methods that can align such networks.

The question is: how to align dynamic networks, when the existing NA methods can only deal with static networks? To allow for this, we generalize the notion of static NA to its dynamic counterpart. Namely, we define *dynamic NA* as a process of comparing dynamic networks and finding similar regions between such networks, while exploiting the temporal information explicitly (unlike static NA, which ignores this information). We hypothesize that aligning dynamic network representations of evolving real-world systems will produce superior alignments compared to aligning the systems' static network representations, as is currently done. To test this hypothesis, we introduce the first ever method for dynamic NA.

Our proposed dynamic NA method, DynaMAGNA++, is a proof-of-concept extension of a state-of-the-art static NA method, MAGNA++ (Vijayan *et al.*, 2015). Saraph and Milenković (2014) and Vijayan *et al.* (2015) compared MAGNA++ to state-of-the-art static NA methods at the time: IsoRank (Singh *et al.*, 2007), MI-GRAAL (Kuchaiev and Pržulj, 2011), and GHOST (Patro and Kingsford, 2012). The comparisons were made on synthetic as well as real-world PINs, in terms of both topological and functional alignment quality. MAGNA++ resulted in higher-quality alignments than the other methods in all of the comparison tests. More recently, Meng *et al.* (2016b) compared in the same manner MAGNA++ to additional newer static NA methods: NETAL (Neyshabur *et al.*, 2013), GEDEVO (Ibragimov *et al.*, 2013),

WAVE (Sun *et al.*, 2015), and L-GRAAL (Malod-Dognin and Pržulj, 2015). On synthetic networks, only MAGNA++ and WAVE produced high-quality alignments across all comparison tests, unlike the other methods. On real-world PINs, the best method varied depending on the comparison test, but overall, MAGNA++ and L-GRAAL produced the highest-quality alignments in most of the tests. Hence, MAGNA++ was the only top-performing method for both synthetic and real-world networks. This is exactly why we have chosen to extend MAGNA++ rather than some other static NA method to its dynamic counterpart. However, as any future static NA methods are developed (Mamano and Hayes, 2017) that are potentially superior to MAGNA++, our ideas on dynamic NA will be applicable to such methods too. Section 2 describes the method, and Section 3 confirms our hypothesis that dynamic NA is superior to static NA, under fair comparison conditions, on both synthetic and real-world networks, and on data from both computational biology and social network domains.

2 Materials and methods

We first describe MAGNA++ and then its DynaMAGNA++ extension.

2.1 MAGNA ++

Static networks and static NA. A static network $G(V, E)$ consists of a node set V and an edge set E. An edge $(u, v) \in E$ is an interaction between nodes u and v. There can only be a single edge between the same pair of nodes. Given two static networks $G_1(V_1, E_1)$ and $G_2(V_2, E_2)$, assuming without loss of generality that $|V_1| \leq |V_2|$, a static NA between G_1 and G_2 is a one-to-one node mapping $f : V_1 \rightarrow V_2$, which produces the set of aligned node pairs $\{(v, f(v)) | v \in V_1\}$ (Fig. 1a).

Static edge conservation. Given an NA between two static networks, an edge in one network is *conserved* if it maps to an edge in the other network, and an edge in one network is *non-conserved* if it maps to a non-adjacent node pair (i.e. a non-edge) in the other network (Fig. 1a). A good static NA is a node mapping that conserves similar network regions. That is, a good static NA should have a large number of conserved edges and a small number of non-conserved edges. In this context, we measure the quality of a static NA using the popular symmetric substructure score (S^3) edge conservation measure (Saraph and Milenković, 2014).

S^3 is defined as follows. Formally, the number of conserved edges is

$$N_c = \sum_{(u,v) \in V_1 \otimes V_1} \mathbb{1}[(u, v) \in E_1 \wedge (f(u), f(v)) \in E_2],$$

and the number of non-conserved edges is

$$N_n = \sum_{(u,v) \in V_1 \otimes V_1} \mathbb{1}[((u, v) \in E_1 \wedge (f(u), f(v)) \notin E_2) \vee$$

$$((u, v) \notin E_1 \wedge (f(u), f(v)) \in E_2)]$$

$$= |E_1| + |E_2'| - 2N_c,$$

where $G_2'(V_2', E_2')$ is the subgraph of G_2 induced by $V_2' = \{f(u) | u \in V_1\}$, $\mathbb{1}[p] = \mathbb{1}$ if p is true and $\mathbb{1}[p] = 0$ if p is false, and $U \otimes V$ is the Cartesian product of sets U and V.

Then, $S^3 = \frac{N_c}{N_c + N_n}$. Supplementary Algorithm S1 describes our S^3 implementation that has $O(|E_1| + |E_2|)$ time complexity.

Static node conservation. A good static NA should also conserve the similarity between aligned node pairs, i.e. node conservation. Node conservation accounts for similarities between all pairs of
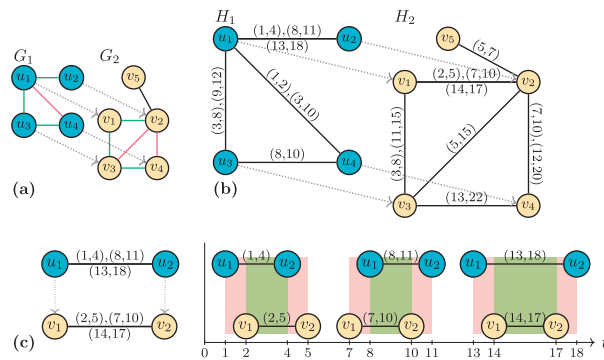
Fig. 1. (a) Two static networks $G_1(V_1, E_1)$ and $G_2(V_2, E_2)$ (where edges be-
tween nodes in the same network are denoted by solid lines), and a static NA
between them (in this case, u_i maps to v_i for $i = 1, \ldots, 4$, as shown by the dot-
ted arrows). An edge is conserved if it maps to another edge (e.g. edge (u_1,
u_2) maps to edge (v_1, v_2)). An edge is non-conserved if it maps to a non-adja-
cent (disconnected) node pair (e.g. edge (u_1, u_4) maps to a disconnected node
pair (v_1, v_4)). All conserved edges are shown in green, and all non-conserved
edges are shown in red. (b) Two dynamic networks $H_1(V_1, T_1)$ and $H_2(V_2, T_2)$.
If two nodes interact at least once during the network's lifetime (i.e. if there is
at least one event between the nodes), there is a solid line between the nodes.
A given solid line can capture multiple events. Each event is represented as
(t_s, t_e), where t_s is its start time, and t_e is its end time. For example, the event
between u_3 and u_4 is active from start time 8 to end time 10. A dynamic NA is
a node mapping between the two networks (in this case, u_i maps to v_i for
$i = 1, \ldots, 4$, as shown by the dotted arrows). (c) Illustration of the conserved
event time (CET) and non-conserved event time (NCET) of the mapping of
node pair (u_1, u_2) to node pair (v_1, v_2). On the left are node pair (u_1, u_2) from
dynamic network $H_1(V_1, T_1)$ and node pair (v_1, v_2) from dynamic network
$H_2(V_2, T_2)$, where (u_1, u_2) maps to (v_1, v_2). For each of the two node pairs (u_1,
u_2) and (v_1, v_2), the event times of the given node pair are visualized by the
plot on the right, where the given solid line in the plot indicates the start time
to the end time of the given event (i.e. the period of time during which the
given node pair is active). Given the above, the CET between (u_1, u_2) and (v_1,
v_2) is the amount of time during which both (u_1, u_2) and (v_1, v_2) are active at
the same time (the green area). Similarly, the NCET between (u_1, u_2) and (v_1,
v_2) is the amount of time during which exactly one of (u_1, u_2) or (v_1, v_2) is ac-
tive (the red area). We calculate the CET between these two illustrated node
pairs as follows. Since the events (u_1, u_2, 1, 4) and (v_1, v_2, 2, 5) are both active
from time 2 to time 4 for a duration of $4 - 2 = 2$, the events (u_1, u_2, 8, 11) and
(v_1, v_2, 7, 10) are both active from time 8 to time 10 for a duration of
$10 - 8 = 2$, and the events (u_1, u_2, 13, 18) and (v_1, v_2, 14, 17) are both active
from time 14 to time 17 for a duration of $17 - 14 = 3$, the total CET between
(u_1, u_2) and (v_1, v_2) is $2 + 2 + 3 = 7$. We calculate the NCET between these two
illustrated node pairs as follows. We know that (u_1, u_2) is active during time
periods 1 to 4, 8 to 11, and 13 to 18, totaling a duration of
$(4 - 1) + (11 - 8) + (18 - 13) = 11$, and that ($v_1$, v_2) is active during time peri-
ods 2 to 5, 7 to 10, and 14 to 17, totaling a duration of
$(5 - 2) + (10 - 7) + (17 - 14) = 9$. Since NCET is the amount of time during
which (u_1, u_2) is active, or (v_1, v_2) is active, but not both, we need to add up
the time during which either node pair is active, and subtract the time during
which both node pairs are active (making sure to subtract twice to avoid dou-
ble counting, because of the "but not both" constraint). Since the time during
which both node pairs are active is the CET, the NCET between (u_1, u_2) and
(v_1, v_2) is $11 + 9 - 2 \times 7 = 6$

nodes across the two networks. Node similarity can be defined in a
way that depends on one's goal or domain knowledge. In this work,
we use a node similarity measure that is based on graphlets, as
follows.

Graphlets (in the static setting) are small, connected, induced
subgraphs of a larger static network (Milenković and Pržulj, 2008).
Graphlets can be used to describe the extended network neighbor-
hood of a node in a static network via the node's graphlet degree
vector (GDV). The GDV generalizes the degree of the node, which

counts how many edges are incident to the node, i.e. how many
times the node touches an edge (where an edge is the only graphlet
on two nodes), into the vector of graphlet degrees (i.e. GDV), which
counts how many times the node touches each of the graphlets on
up to n nodes, accounting in the process for different topologically
unique node symmetry groups (automorphism orbits) that might
exist within the given graphlet. In this work, we use all graphlets
with up to four nodes, which contain 15 automorphism orbits,
when calculating the GDV of a node, per recommendations of the
existing studies (Hulovatyy *et al.*, 2015, 2014). Hence, the GDV of
a node has 15 dimensions containing counts for the 15 orbits.

Given GDVs of all nodes in two static networks $G_1(V_1, E_1)$ and
$G_2(V_2, E_2)$, where x_u is the GDV of node u, we calculate similarity
$s(u, v)$ between nodes $u \in V_1$ and $v \in V_2$ by relying on an existing
GDV-based measure of node similarity that was used by Hulovatyy
et al. (2015). The measure works as follows. First, to extract GDV
dimensions that contain the most relevant information about the ex-
tended network neighborhood of the given node, the measure re-
duces dimensionality of each GDV via principal component analysis
(PCA). PCA is performed on the vector set $\{x_w | w \in V_1 \cup V_2\}$, where
we keep as few of the first k PCA components as needed to account
for at least 99% of variance in the vector set. Let us denote by y_u the
dimensionality-reduced vector of x_u that contains the k PCA compo-
nents. Second, we define node similarity $s(u, v)$ as the cosine similar-
ity between y_u and y_v. Third, given a static NA f, we define our node
conservation measure as $\sum_{u \in V_1} \frac{s(u, f(u))}{|V_1|}$.

Objective function and optimization process (or search strategy).
MAGNA++ is a search-based algorithm that finds a static NA by
directly maximizing both edge and node conservation. Namely, it
maximizes the objective function $\alpha S_E + (1 - \alpha)S_N$, where S_E is the
S^3 measure of static edge conservation described above, S_N is the
graphlet-based measure of static node conservation described above,
and α is a parameter between 0 and 1 that controls for the two meas-
ures. In several studies, it was shown that α of 0.5 yields the best re-
sults (Meng *et al.*, 2016b; Vijayan *et al.*, 2015), which is the α value
we use in this study, unless otherwise noted. Given an initial popula-
tion of random static NAs, MAGNA++ evolves the population of
alignments over a number of generations while aiming to maximize
its objective function. MAGNA++ then returns the alignment from
the final generation that has the highest value of the objective
function.

2.2 DynaMAGNA++

Dynamic networks. A *dynamic network* $H(V, T)$ consists of a node
set V and an event set T, where an event is a temporal edge (Fig. 1b).
An event is a 4-tuple (u, v, t_s, t_e), where nodes u and v interact from
time t_s to time t_e. An event is *active* at time t if $t_s \leq t \leq t_e$. The *dur-
ation* of an event is the time during which an event is active, i.e.,
$t_e - t_s$. There can be multiple events between the same two nodes in
the dynamic network, but no two events between the same two
nodes may be active at the same time. In fact, if there are two events
between the same two nodes that are active at the same time, then
they must be combined into a single event.

In the above representation of a dynamic network that our NA
method uses, time is captured in a continuous manner (i.e. each
event has a duration). However, dynamic network data is often pro-
vided in a different representation, as a discrete temporal sequence
of static network snapshots $G_1(V_1, E_1), \ldots, G_k(V_k, E_k)$. We can eas-
ily convert the static snapshot-based representation of a dynamic net-
work into our event duration-based representation (i.e. into $H(V, T)$
as defined above). We do this as follows: if there is an edge

connecting two nodes in the tth snapshot of the snapshot-based representation, then there is an event between the two nodes that is active from time t to time $t+1$ in the event duration-based representation. In other words, we combine the node sets of the snapshots into a single node set $V = V_1 \cup \ldots \cup V_k$. Then, for each snapshot G_t, $t = 1, \ldots, k$, we convert each edge $(u, v) \in E_t$ into an event between nodes $u \in V$ and $v \in V$ in the dynamic network $H(V, T)$ with start time t and end time $t+1$, i.e., the event $(u, v, t, t+1)$. This allows us to use the snapshot-based representation of a dynamic network in our study.

Dynamic NA. Given two dynamic networks $H_1(V_1, T_1)$ and $H_2(V_2, T_2)$, assuming without loss of generality that $|V_1| \leq |V_2|$, a *dynamic NA* between H_1 and H_2 is a one-to-one node mapping $f : V_1 \to V_2$, which produces the set of aligned node pairs $\{(v, f(v)) \mid v \in V_1\}$ (Fig. 1b). Note the similarity between the definitions of static NA and dynamic NA (although the process of finding the actual alignments is different). This makes static NA and dynamic NA fairly comparable.

Dynamic edge (event) conservation. First, given node pair (u_1, u_2) in H_1 that maps to node pair (v_1, v_2) in H_2 (Fig. 1c), we extend the notion of a conserved or non-conserved edge from static NA to dynamic NA by accounting for the amount of time that the mapping of (u_1, u_2) to (v_1, v_2) is conserved or non-conserved (defined below). That is, we extend the notion of a conserved or non-conserved static edge to the amount of a conserved or non-conserved dynamic edge (event), as follows.

We define the amount of a conserved event as follows. Similar to how an edge (u'_1, u'_2) in static network $G_1(V_1, E_1)$ is conserved if it maps to an edge (v'_1, v'_2) in static network $G_2(V_2, E_2)$ (and vice versa), the mapping of (u_1, u_2) to (v_1, v_2) is *conserved* at time t if both (u_1, u_2) and (v_1, v_2) are active at time t. We refer to the entire amount of time during which this mapping is conserved as the *conserved event time (CET)* between (u_1, u_2) and (v_1, v_2). In other words, it is the amount of time during which both (u_1, u_2) and (v_1, v_2) are active at the same time. Formally, let $T_{u_1 u_2}$ be the set of events between u_1 and u_2, and let $T_{v_1 v_2}$ be the set of events between v_1 and v_2. Then, the CET between (u_1, u_2) and (v_1, v_2) is

$$\text{CET}((u_1, u_2), (v_1, v_2)) = \sum_{e \in T_{u_1 u_2}} \sum_{e' \in T_{v_1 v_2}} ct(e, e'),$$

where the conserved time $ct(e, e') = \max(0, \min(t_e, t'_e) - \max(t_s, t'_s))$ is the amount of time during which events $e = (u_1, u_2, t_s, t_e)$ and $e' = (v_1, v_2, t'_s, t'_e)$ are active at the same time, i.e., $ct(e, e')$ is the length of the overlap of the intervals $[t_s, t_e]$ and $[t'_s, t'_e]$.

We define the amount of a non-conserved event as follows. Similar to how an edge (u'_1, u'_2) in G_1 is non-conserved if it maps to a disconnected node pair (v'_1, v'_2) in G_2 (or vice versa), the mapping of (u_1, u_2) to (v_1, v_2) is *non-conserved* at time t if exactly one of (u_1, u_2) or (v_1, v_2) is active at time t. We refer to the entire amount of time during which this mapping is non-conserved as the *non-conserved event time (NCET)* between (u_1, u_2) and (v_1, v_2). In other words, it is the amount of time during which (u_1, u_2) is active, or (v_1, v_2) is active, but not both are active at the same time. Formally, the NCET between (u_1, u_2) and (v_1, v_2) is

$$\text{NCET}((u_1, u_2), (v_1, v_2))$$
$$= \sum_{e \in T_{u_1 u_2}} d(e) + \sum_{e' \in T_{v_1 v_2}} d(e') - 2 \sum_{e \in T_{u_1 u_2}} \sum_{e' \in T_{v_1 v_2}} ct(e, e'),$$

where $d(e)$ is the duration of event e, i.e., the amount of time during which e is active. We make sure to subtract twice the amount of

time during which (u_1, u_2) and (v_1, v_2) are both active due to the above "but not both are active at the same time" constraint.

Second, given these definitions of CET and NCET between two node pairs (u_1, u_2) and (v_1, v_2), we extend the S^3 measure of static edge conservation to a new dynamic S^3 (DS^3) measure of dynamic edge (event) conservation. To define DS^3, we need to introduce the notion of CET between all node pairs across the entire alignment (rather than between just two aligned node pairs), henceforth simply referred to as *alignment CET*, which is the sum of CET between all node pair mappings between H_1 and H_2. Also, we need to define the notion of *alignment NCET*, which is the sum of NCET between all node pair mappings between H_1 and H_2. Alignment CET measures the amount of event conservation of the entire alignment and alignment NCET measures the amount of event non-conservation of the entire alignment. A good dynamic NA is a node mapping that conserves similar evolving network regions. That is, a good dynamic NA should have high alignment CET and low alignment NCET, which is what DS^3 aims to capture. Formally, alignment CET is

$$T_c = \sum_{(u, v) \in V_1 \otimes V_1} \text{CET}((u, v), (f(u), f(v)))$$

and alignment NCET is

$$T_n = \sum_{(u, v) \in V_1 \otimes V_1} \text{NCET}((u, v), (f(u), f(v))).$$

Then, $DS^3 = \frac{T_c}{T_c + T_n}$. Supplementary Algorithm S2 describes our DS^3 implementation that has $O(|T_1| + |T_2|)$ time complexity.

We note that there are many real-world networks that contain events with durations that are significantly less than the entire time window of the network, called "bursty" events. Examples of networks containing bursty events are e-mail communication networks, economic networks that model transactions, and brain networks constructed from oxygen level correlations as measured by fMRI scanning, each of whose events last much less than a second while the networks' time windows span minutes to hours (Holme, 2015). Since bursty events are so short, small perturbations in the event times can greatly affect the resulting dynamic edge (event) conservation value. Thus, in order to allow our DS^3 measure to be more robust to perturbations of up to Δt in the event times, one may simply extend the duration of each event in the network by $2\Delta t$. This is due to the following. Given two events (u_1, u_2, t, t) and (v_1, v_2, t', t') with durations of 0, where $t' = t + \Delta t$, the conserved time $ct(\cdot, \cdot)$ between the two events is 0. Thus, if we want to consider the two events as conserved, we can increase the durations of both events by $2\Delta t$ to create the modified events $(u_1, u_2, t - \Delta t, t + \Delta t)$ and $(v_1, v_2, t' - \Delta t, t' + \Delta t)$, which results in a conserved time of Δt for the two modified events. While we do not use this technique in our work since we do not use networks with bursty events, others might in the future, and if so, this needs to be considered when performing dynamic NA.

Dynamic node conservation. Just as for static NA, a good dynamic NA method should also conserve the similarity between aligned node pairs, i.e. node conservation. To take advantage of the temporal information encoded in dynamic networks that are being aligned and also to make dynamic NA as fairly comparable as possible to static NA, in this work, we rely on a measure of node similarity based on dynamic graphlets, as follows.

Dynamic graphlets are an extension of static graphlets (Section 2.1) to the dynamic setting. While static graphlets can be used to capture the static extended network neighborhood of a node, dynamic graphlets can be used to capture how the extended

neighborhood of a node changes over time. To define dynamic graphlets, we first present the notion of a Δt-time-respecting path and a Δt-connected network. A Δt-time-respecting path is a sequence of events that connect two nodes such that for any two consecutive events in the sequence, the end time of the earlier event and the start time of the later event are within Δt time of each other (i.e., are Δt-adjacent). A dynamic network is Δt-connected if for each pair of nodes in the network, there is a Δt-time-respecting path between the two nodes. Then, just as a static graphlet is an equivalence class of isomorphic connected subgraphs (Section 2.1), a *dynamic graphlet* is an equivalence class of isomorphic Δt-connected dynamic subgraphs, where two graphlets are equivalent if they both have the same *relative* temporal order of events. We use $\Delta t = 1$, per recommendations by Hulovatyy *et al.* (2015). Just as the GDV of a node in a static network is a topological descriptor for the extended neighborhood of the node, there exists the *dynamic GDV (DGDV)* of a node in a dynamic network, which describes how the extended neighborhood of a node changes over time. Specifically, just as the GDV of a node counts how many times the node touches each static graphlet at each of its automorphism orbits, the DGDV of a node counts how many times the node touches each dynamic graphlet at each of its orbits. Dynamic graphlets have a similar notion of orbits as static graphlets do, which now depend on both topological and temporal positions of a node within the dynamic graphlet. To make things fairly comparable to static NA, and per recommendations by Hulovatyy *et al.* (2015), we use dynamic graphlets with up to four nodes and six events, which contain 3727 automorphism orbits. Hence, the DGDV of a node has 3727 dimensions containing counts for the 3727 orbits.

Given the DGDVs of all nodes in two dynamic networks $H_1(V_1, T_1)$ and $H_2(V_2, T_2)$, just as in Section 2.1, we calculate similarity $s(u, v)$ between nodes $u \in V_1$ and $v \in V_2$ and then rely on cosine similarities between the PCA-based dimensionality-reduced DGDVs to obtain the total dynamic node conservation.

Objective function and optimization process (also known as search strategy). DynaMAGNA++ is a search-based algorithm that finds a dynamic NA by directly maximizing both dynamic edge (event) and node conservation. Namely, DynaMAGNA++ maximizes the objective function $\alpha S_T + (1 - \alpha)S_N$, where S_T is the DS^3 measure of dynamic edge conservation described above, S_N is the DGDV-based measure of dynamic node conservation described above, and α is a parameter between 0 and 1 that controls for the two measures. To make DynaMAGNA++ fairly comparable to MAGNA++, here we also use MAGNA++'s best α value of 0.5, unless otherwise noted. Given an initial population of random dynamic NAs, DynaMAGNA++ evolves the population of alignments over a number of generations while aiming to maximize its objective function. DynaMAGNA++ then returns the alignment from the final generation that has the highest value of the objective function.

Time complexity. To align two dynamic networks $H_1(V_1, T_1)$ and $H_2(V_2, T_2)$, DynaMAGNA++ evolves a population of p alignments over N generations. It does so by using its crossover function (see Saraph and Milenković (2014) for details) to combine pairs of parent alignments in the given population into child alignments, for each generation. For each generation, the dynamic edge (event) conservation, dynamic node conservation, and crossover of $O(p)$ alignments are calculated. Since dynamic edge conservation takes $O(|T_1| + |T_2|)$ to compute, dynamic node conservation takes $O(|V_1|)$ time to compute, crossover takes $O(|V_2|)$ time to compute, and $|V_1| \leq |V_2|$, the time complexity of DynaMAGNA++ is $O(Np|V_2| + Np(|T_1| + |T_2|))$. Note that the calculation of dynamic edge and dynamic node conservation in DynaMAGNA++ is

parallelized. This allows DynaMAGNA++ to be run on multiple cores, which empirically results in close to linear speedup.

Other parameters. Given an initial population of dynamic NAs, DynaMAGNA++ evolves the population for up to a specified number of generations or until it reaches a stopping criterion. For each generation, DynaMAGNA++ keeps an elite fraction of alignments from the current generation's population for the next generation's population. In addition to the dynamic edge and node conservation measures, and the α parameter that controls for the contribution of the two measures, the remaining parameters of DynaMAGNA++ are (i) the initial population, (ii) the size of the population, (iii), the maximum number of generations, (iv) the elite fraction, and (v) the stopping criterion. For DynaMAGNA++, we use a population of 15 000 alignments initialized randomly, as in the original MAGNA++ paper. We specify a maximum of 10 000 generations, since the alignments that we test all converge by 10 000 generations. The elite fraction is 0.5, as in the original MAGNA++ paper. The algorithm stops when the highest objective function value in the population has increased less than 0.0001 within the last 500 generations, since the alignments that we test do not increase by a significant amount after this point.

To fairly compare DynaMAGNA++ against MAGNA++, we aim to set the parameters of both methods to be as similar as possible. So, other than MAGNA++'s edge and node conservation measures, the remaining parameters of MAGNA++ are the same as for DynaMAGNA++. This way, any differences that we see between results of DynaMAGNA++ and results of MAGNA++ will be the consequence of the differences of the two methods' edge and node conservation measures, i.e. of accounting for temporal information in the network with DynaMAGNA++ and ignoring this information with MAGNA++. In other words, any differences that we see between results of DynaMAGNA++ and results of MAGNA++ will fairly reflect differences between dynamic NA and static NA.

3 Results and discussion

Since there are no other dynamic NA methods to compare against, we compare DynaMAGNA++ to the next best option, namely its static NA counterpart. That is, we compare DynaMAGNA++ when it is used to align two dynamic networks, to MAGNA++ when it is used to align static versions of the two dynamic networks. By "static versions", we mean that we "flatten" or "aggregate" a dynamic network into a static network that will have the same set of nodes as the dynamic network and a static edge will exist between two nodes in the static network if there is at least one event between the same two nodes in the dynamic network. This network aggregation simulates the common practice where network analysis of time-evolving systems is done in a static manner, by ignoring their temporal information (Holme, 2015). We evaluate DynaMAGNA++ and MAGNA++ on synthetic and real-world dynamic networks, as follows.

3.1 Evaluation using synthetic networks
Motivation. A good NA approach should be able to produce high-quality alignments between networks that are similar and low-quality alignments between networks that are dissimilar (Yaveroğlu *et al.*, 2015). In this test on synthetic networks, "similar" means networks that originate from the same network model, and "dissimilar" means networks that originate from different network models. So, we refer to this test as network discrimination. Thus, in this

section, we evaluate the network discrimination performance of DynaMAGNA++ and MAGNA++.

Data. We perform this evaluation on a set of biologically inspired synthetic networks. Specifically, we generate 20 dynamic networks using four biologically inspired network evolution models (or versions of the same model with different parameter values) that simulate the evolution (i.e. growth) of PINs, resulting in five networks per model (Hulovatyy *et al.*, 2015). The four models that we use are (i) GEO-GD with $p = 0.3$, (ii) GEO-GD with $p = 0.7$, (iii) SF-GD with $p = 0.3$ and $q = 0.7$, and (iv) SF-GD with $p = 0.7$ and $q = 0.6$, where GEO-GD is a geometric gene duplication model with probability cut-off and SF-GD is a scale-free gene duplication model (Pržulj *et al.*, 2010). Hulovatyy *et al.* (2015) generalized the static versions of these models to their dynamic counterparts, and we rely on the same model networks as those used by Hulovatyy *et al.* (2015) (see their paper for details). Intuitively, each of the 20 synthetic networks is represented as a sequence of snapshots, where snapshot size increases with time, as illustrated in Supplementary Figure S1. The final (largest) snapshot of each synthetic network has 1000 nodes, and the number of edges varies depending on the different parameter values of the considered network models. Representative statistics describing the final snapshot of each of the synthetic networks, such as their sizes or degree distributions, are shown in Supplementary Table S1 and Supplementary Figure S2.

To illustrate generalizability of dynamic NA to other domains, we also perform this evaluation on a set of social synthetic networks generated using different parameter values of a social network evolution model (due to space constraints, we refer the reader to Supplementary Section S1.1, Supplementary Table S2, and Supplementary Figs S3–S4 for details).

Evaluation measures. We calculate performance of each method as follows. We align all possible pairs of the synthetic networks. The higher the alignment quality between pairs of similar networks (i.e. networks coming from the same model) and the lower the alignment between pairs of dissimilar networks (i.e. networks coming from different models), the better the NA method. Here, by alignment quality between two networks that the given method identifies, we mean the method's objective function value for the alignment of the two networks that is returned by the method (Section 2). Given the alignment quality values for all network pairs, we summarize the given method's performance using precision-recall and receiver operating characteristic (ROC) frameworks. For some given threshold r, a good NA method should result in alignment quality greater than r for pairs of similar networks and in alignment quality smaller than r for pairs of dissimilar networks. So, for a given threshold r, we compute accuracy in terms of precision, the fraction of network pairs that are similar and with alignment quality greater than r out of all network pairs with alignment quality greater than r, and recall, the fraction of network pairs that are similar and with alignment quality greater than r out of all similar network pairs. Varying the threshold r for all $r \geq 0$ (i.e. for r between 0 and the maximum observed alignment quality value, in increments of the smallest difference between any pair of observed alignment quality values) gives us the precision-recall curve. Then, we compute the area under the precision-recall curve (AUPR), the F-score (harmonic mean of precision and recall) at which precision and recall cross and are thus equal (F-score$_{cross}$), and the maximum F-score over all threshold r values (F-score$_{max}$). For a given threshold r, we also compute method accuracy in terms of sensitivity, which is the same as recall, and specificity, the fraction of network pairs that are dissimilar and with alignment quality less than r out of all network pairs that are dissimilar. Varying the threshold r for all $r \geq 0$ gives us the receiver

operating characteristic (ROC) curve. Then, we compute the area under the ROC curve (AUROC).

Results. First, we aim to test whether optimizing both dynamic edge (event) conservation and dynamic node conservation in DynaMAGNA++ is better than optimizing either dynamic edge conservation alone or dynamic node conservation alone, since it was shown for MAGNA++ that optimizing both static edge conservation and static node conservation performs better than optimizing any one of static edge conservation or static node conservation alone (Meng *et al.*, 2016b; Vijayan *et al.*, 2015). So, we compare three different versions of DynaMAGNA++ that differ in their optimization functions. The three versions optimize: (i) a combination of dynamic edge conservation and dynamic node conservation (corresponding to $\alpha = 0.5$, named DynaMAGNA++ (E+N)), (ii) dynamic edge conservation only (corresponding to $\alpha = 1$, named DynaMAGNA ++ (E)), and (iii) dynamic node conservation only (corresponding to $\alpha = 0$, named DynaMAGNA++ (N)) (Section 2). We find that while DynaMAGNA++ (N) performs the best for biological synthetic networks (Table 1, Supplementary Fig. S5, and Supplementary Table S3), it performs the worst for the social synthetic networks (Table 2, Supplementary Fig. S6, and Supplementary Table S4). Similarly, DynaMAGNA++ (E) performs the best for synthetic social networks (Table 2) but the worst for biological synthetic networks (Table 1). On the other hand, DynaMAGNA++ (E+N) consistently performs well (though not the best) in both cases. Because of this, and because DynaMAGNA++ (E+N) is the best of all three versions for all analyzed real-world networks (as we show in Section 3.2), in the main paper, we only report results for DynaMAGNA++ (E+N) and refer to it simply as DynaMAGNA++. We report results for DynaMAGNA++ (E) and DynaMAGNA++ (N) in the Supplement (Supplementary Section S1.2). This way, we fairly compare DynaMAGNA++ and MAGNA++, both using $\alpha = 0.5$.

Second, and most importantly, we test whether dynamic NA is superior to static NA, by comparing the network discrimination performance of DynaMAGNA++ and MAGNA++. Indeed, for biological synthetic networks, DynaMAGNA++ outperforms MAGNA++ with respect to all considered NA quality measures (Fig. 2, Table 3, Supplementary Fig. S5, and Supplementary Table S3). Similar results (superiority of DynaMAGNA++ over MAGNA++) also hold for the social synthetic networks (Supplementary Fig. S6 and Supplementary Table S4).

In summary, under fair comparison conditions, we demonstrate that dynamic NA is superior to static NA for synthetic dynamic networks.

3.2 Evaluation using real-world networks

Motivation. Here, we still evaluate whether the given method produces high-quality alignments for similar networks and low-quality
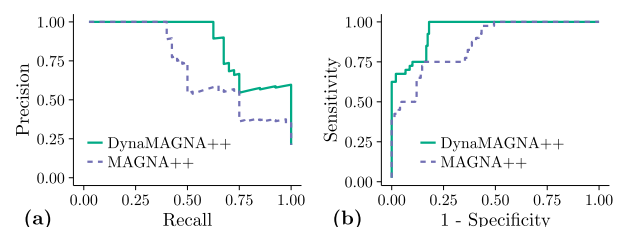

Fig. 2. Network discrimination performance of DynaMAGNA++ and MAGNA++ for biological synthetic networks with respect to **(a)** precision-recall curve and **(b)** ROC curve

Table 1. Network discrimination performance of DynaMAGNA++, while optimizing both dynamic edge and node conservation (E + N), dynamic edge conservation alone (E), and dynamic node conservation alone (N), for *biological* synthetic networks, with respect to the area under the precision-recall curve (AUPR), F-score at which precision and recall cross and are thus equal (F-score$_{cross}$), maximum F-score (F-score$_{max}$), and the area under the ROC curve (AUROC)

NA method	AUPR	F-score$_{cross}$	F-score$_{max}$	AUROC
DynaMAGNA++ (E+N)	0.865	0.700	0.771	0.950
DynaMAGNA++ (E)	0.742	0.550	0.762	0.919
DynaMAGNA++ (N)	**0.994**	**0.950**	**0.962**	**0.998**

Note: In each column, the highest score is bolded.

Table 2. Equivalent of Table 1 for *social* synthetic networks

NA method	AUPR	F-score$_{cross}$	F-score$_{max}$	AUROC
DynaMAGNA++ (E+N)	0.908	0.800	0.839	0.959
DynaMAGNA++ (E)	**1.000**	**1.000**	**1.000**	**1.000**
DynaMAGNA++ (N)	0.751	0.600	0.723	0.883

Note: In each column, the highest score is bolded.

Table 3. Network discrimination performance of DynaMAGNA++ and MAGNA++, for biological synthetic networks, with respect to the same measures as in Table 1

NA method	AUPR	F-score$_{cross}$	F-score$_{max}$	AUROC
DynaMAGNA++	**0.865**	**0.700**	**0.771**	**0.950**
MAGNA++	0.711	0.550	0.645	0.863

Note: In each column, the highest score is bolded.

alignments for dissimilar networks. However, the notion of similarity that we use here is different than for the synthetic networks above, because for real-world networks, we do not know which network models they belong to (Yaveroğlu *et al.*, 2015). Specifically, we align an original real-world network to its randomized (noisy) versions (see below), where we vary the noise level. The larger the noise level, the more dissimilar the aligned networks are, and thus, the lower the alignment quality should be.

Zebra network. Since there is a lack of available dynamic *molecular* networks (Section 1), we begin our evaluation of real-world networks on an alternative biological network type — an ecological network. The original real-world network that we use is the Grevy's zebra proximity network (Rubenstein *et al.*, 2015), which contains information on interactions between 27 zebras in Kenya over 58 days. The data was collected by driving a predetermined route each day while searching for herds. There are 779 events in the network. We also report results for another animal proximity network that contains information on interactions between 28 onagers, a species that is closely related to the Grevy's zebra, mostly in the Supplement due to space constraints (Supplementary Section S1.3). The onager proximity network contains 28 nodes and 522 events.

Since the difference between dynamic NA and static NA is that the former accounts for the temporal aspect of the data more explicitly than the latter, to properly validate results for dynamic NA, as strict randomization scheme as possible should be used when creating randomized (noisy) versions of the original dynamic network that will be aligned to the original network. By "as strict as possible", we mean that we want to use a randomization scheme that preserves as much structure (i.e. topology) as possible of the

dynamic network and randomizes only the temporal aspect of the network. This way, the only difference observed between DynaMAGNA++'s and MAGNA++'s performance will be the consequence of considering the temporal aspect of the data. For this reason, we randomize the original network using the following model per recommendations by Holme (2015). In order to randomize the original dynamic network $H(V, T)$ to a certain noise level, first, we arbitrarily number all m events in the network as $T = \{e_1, e_2, \ldots, e_m\}$. Then, for each event e_i, with probability p (where p is the noise level) we randomly select another event $e_j, j \neq i$, and swap the time stamps of the two events. Since we only swap the time stamps, this randomization scheme conserves the total number of events and the structure of the flattened version of the original dynamic network. We study 10 different noise levels, from 0% to 100% in smaller increments initially and larger increments toward the end (clearly, at the 0% noise level, the aligned networks are identical). For each noise level, we generate five randomized versions of the original network and report results averaged over the five randomization runs.

We evaluate DynaMAGNA++ and MAGNA++'s performance as follows. First, for a good method, alignment quality should decrease as the noise level increases, since the original network and its randomized version become more dissimilar with this increase. As in Section 3.1, one measure of alignment quality that we use is each method's objective function. Another measure that we use is node correctness. Node correctness of an alignment is the fraction of correctly aligned node pairs (according to the ground truth node mapping) out of all aligned node pairs. Given that our original network and its randomized versions have the same set of nodes, we know which nodes in the original network correspond to which nodes in the given randomized network. That is, we know the ground truth (or perfect) mapping between the aligned networks. Hence, we can measure node correctness between the networks. Thus, we evaluate each method's alignment quality using the method's objective function as well as node correctness, with the expectation that for a good method, alignment quality should decrease with increase in the noise level.

Second, since we know the perfect alignment between the original network and each of its randomized versions, we compute the "ideal" alignment quality — the quality of the perfect alignment, as measured by DynaMAGNA++'s objective function. The expectation is that a good method's alignment quality should mimic well the "ideal" quality.

Third, we expect DynaMAGNA++'s alignment quality to be superior to MAGNA++'s alignment quality with respect to node correctness for lower (meaningful) noise levels, if it is indeed true that dynamic NA is superior to static NA. We do not expect this superiority for higher noise levels, since at such noise levels, networks being aligned are highly randomized and thus a good method should produce low-quality alignments.

Indeed, our results confirm all three of the above expectations (Fig. 3 and Supplementary Fig. S7). Specifically, first, DynaMAGNA++'s alignment quality indeed decreases with the increase in the noise level with respect to both its objective function (Fig. 3a) as well as node correctness (Fig. 3b). On the other hand, MAGNA++'s alignment quality stays constant with increase in the noise level. In other words, MAGNA++ produces alignments of the same quality for low noise levels (where network structure is meaningful) as it does for high noise levels (where network structure is random). Second, DynaMAGNA++'s alignment quality follows closely the quality of the perfect alignments, while MAGNA++ does not (Fig. 3a). Third, DynaMAGNA++ achieves higher node

correctness than MAGNA++ at lower (meaningful) noise levels. This is not a surprise, since DynaMAGNA++ explicitly uses the temporal information in the aligned networks, while MAGNA++ does not. Thus, in summary, dynamic NA outperforms static NA. We observe similar results for the onager network (Supplementary Fig. S8).

The above complete failure of MAGNA++ to produce alignments of decreasing quality as the noise level increases is due to the strict randomization scheme that we use to create the noisy versions of the original network, which conserves all structure of the flattened version of the original dynamic network. Recall that we use the strict randomization scheme to ensure that the results of DynaMAGNA++ are meaningful. Yet, to give as fair advantage as possible to static NA, we produce a different set of noisy versions of the original network using a somewhat more flexible randomization scheme that does not conserve the structure of the flattened version of the original dynamic network, per recommendations of Holme (2015). This randomization scheme works as follows. In order to randomize the original dynamic network $H(V, T)$ to a certain noise level, first, we arbitrarily number all m events in the network as $T = \{e_1, e_2, \ldots, e_m\}$. Then, for each event e_i, with probability p (where p is the noise level) we randomly select an event $e_{i'}$, and we rewire the two events. That is, given $e_i = (u, v, t_s, t_e)$ and $e_{i'} = (u', v', t'_s, t'_e)$, we either set $e_i = (u, v', t_s, t_e)$ and $e_{i'} = (u', v, t_s, t_e)$ with probability 0.5, or we set $e_i = (u, u', t_s, t_e)$ and $e_{i'} = (v, v', t_s, t_e)$ with probability 0.5. If the rewiring creates a loop (i.e., an event from a node to itself) or a multiple link (i.e., duplicate events between the same nodes), then we undo it and randomly select another event $e_{i'}$. This randomization scheme conserves the entire set of time stamps of the original network, but it does not preserve the structure of the flattened network. We study 10 different noise levels (from 0% to 100% in smaller increments initially and larger increments toward the end). For each noise level, we generate five randomized versions of the original network and report results averaged over the five randomization runs. While now MAGNA++'s alignment quality also decreases with increase in the noise level and also MAGNA++ closely follows the quality of the perfect alignments, as it should (Fig. 4a and Supplementary Fig. S9), DynaMAGNA++ is still superior to MAGNA++ with respect to node correctness (Fig. 4b), which again implies that dynamic NA is superior to static NA.

Because the results are consistent independent of the randomization scheme that is used to produce noisy networks, and since the strict scheme should be used to correctly evaluate DynaMAGNA++'s correctness, henceforth, we report results only for the strict randomization scheme.
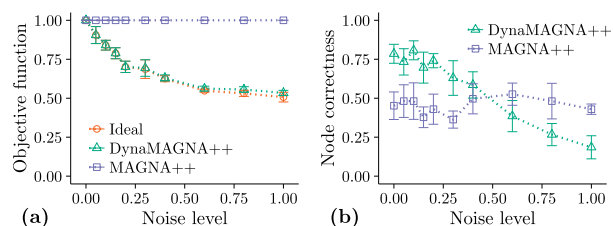
Yeast network. Since there is a lack of available *experimental* dynamic molecular networks, we continue our evaluation of real-world networks on the next best available dynamic molecular network option. Namely, we create a dynamic yeast PIN from an artificial temporal sequence of static yeast PINs. Here, the static PINs that are used as snapshots of the dynamic PIN are all real-world networks, it is just their temporal sequence that is artificial. The sequence consists of six static PIN snapshots: a high-confidence *S. cerevisiae* (yeast) PIN with 1004 proteins and 8323 interactions, and five lower-confidence yeast PINs constructed by adding to the high-confidence PIN 5%, 10%, 15%, 20%, or 25% of lower-confidence interactions; the interactions are added in order of decreasing confidence. Clearly, the five lower-confidence PINs have the same 1004 nodes as the high-confidence PIN, and the largest of the five lower-confidence PINs has 25% more edges than the high-confidence PIN, i.e. 10 403 of them. This network set has been used in many existing static NA studies (Kuchaiev *et al.*, 2010; Milenković *et al.*, 2010; Kuchaiev and Pržulj, 2011; Meng *et al.*, 2016b; Saraph and Milenković, 2014; Vijayan and Milenković, 2016). When we use the six static PINs as snapshots to form a dynamic network, we order the six networks from the smallest one in terms of the number of edges (i.e. the one of the highest confidence) to the largest one in terms of the number of edges (i.e. the one of the lowest confidence). Since each static PIN contains the same set of nodes, this simulates a dynamic network that is growing as it evolves, with more and more interactions being added to the network over time. When we align the resulting (original) dynamic yeast network to its randomized versions, we find that just as for the zebra network, DynaMAGNA++'s alignment quality decreases with increase in the noise level, with respect to both its objective function (Fig. 5a) as well as node correctness (Fig. 5b), while MAGNA++'s alignment quality does not change. Further, DynaMAGNA++ again matches more closely the quality of the perfect alignments than MAGNA++ does (Fig. 5a). Finally, DynaMAGNA++ again produces higher node correctness than MAGNA++ for the lower (meaningful) noise levels. Thus, dynamic NA is superior to static NA for the yeast network as well.

Enron network. To demonstrate DynaMAGNA++'s generalizability on non-biological networks, we continue our evaluation on a social network. The original network that we use is the Enron e-mail communication network (Priebe *et al.*, 2005), which is based on e-mail communications of 184 employees in the Enron corporation from 2000 to 2002, made public by the Federal Energy Regulatory Commission during its investigation. The entire two-year time period is divided into two-month periods so that if there is at least one e-mail sent between two people within a particular two-month period, then there exists an event between the two people during that period. There are 5539 events in the Enron network.
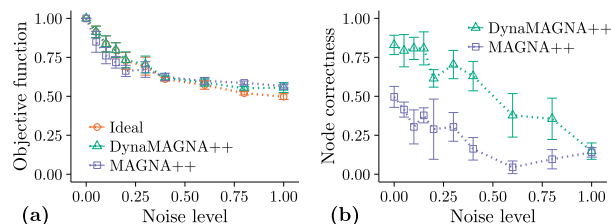
Fig. 3. Alignment quality of DynaMAGNA++ and MAGNA++ as a function of noise level when aligning the original Grevy's zebra network to randomized (noisy) versions of the original network. Here, the randomization is as strict as possible, as it conserves all structure of the flattened version of the original dynamic network and only randomly "shuffles" the given percentage (noise level) of its event time stamps. Alignment quality is shown with respect to **(a)** each method's objective function, and **(b)** node correctness. "Ideal" in panel (a) shows the quality of perfect alignments (see the text)

Fig. 4. Alignment quality of DynaMAGNA++ and MAGNA++ for the Grevy's zebra network. The figure can be interpreted in the same way as Figure 3, except that here, the randomization used to create the noisy networks does not conserve the structure of the flattened version of the original dynamic network
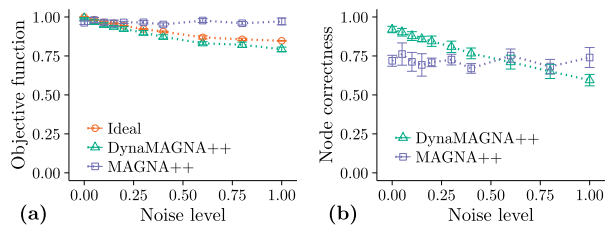
Fig. 5. Alignment quality of DynaMAGNA++ and MAGNA++ for the yeast network. The figure can be interpreted in the same way as Figure 3
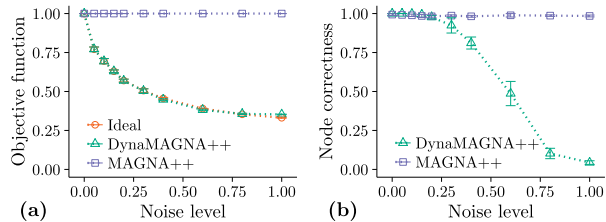

Fig. 6. Alignment quality of DynaMAGNA++ and MAGNA++ for the Enron network. The figure can be interpreted in the same way as Figure 3

When we align the original network to its randomized versions, we find that just as for the zebra and yeast networks, DynaMAGNA++'s alignment quality decreases with increase in the noise level, while MAGNA++'s alignment quality does not change (Fig. 6). Further, DynaMAGNA++ again matches more closely the quality of the perfect alignments (Fig. 6a). So, these results again indicate that dynamic NA is superior to static NA. Interestingly, for this network, MAGNA++ also produces high-quality alignments with respect to node correctness for the low noise levels, just like DynaMAGNA++ does (Fig. 6b).

On optimizing edge versus node conservation for real-world networks. Here, we briefly come back to the discussion of which of DynaMAGNA++ (E+N), DynaMAGNA++ (E), or DynaMAGNA++ (N) is superior. For all analyzed real-world networks, DynaMAGNA++ (E+N) is superior to the other two versions (Table 4), which justifies our choice to mainly report the results of DynaMAGNA++ (E+N) throughout the paper.

Running time. Recall that the time complexity of DynaMAGNA++ is linear with respect to the number of events in the aligned networks (Section 2.2), while the time complexity of MAGNA++ is linear with respect to the number of edges in the aligned networks (Section 2.1). Because there are typically more events in a dynamic network than edges in its flattened version, and because more computations are involved when calculating event conservation than when calculating edge conservation, DynaMAGNA++ is expected to be slower than MAGNA++ (yet, it is this ability of DynaMAGNA++ to capture temporal event information that makes it more accurate than MAGNA++). When using eight cores to align the yeast network to its 0% randomized version, DynaMAGNA++ takes 2.0 hours, with 2% of this time spent on counting dynamic graphlets, while MAGNA++ takes 0.8 hours, with 11% of this time spent of counting static graphlets (faster implementations for static graphlet counting exist (Hočevar and Demšar, 2014)). This makes DynaMAGNA++ 2.5 times slower than MAGNA++. Nonetheless, the somewhat slower (yet still very practical) runtime of DynaMAGNA++ is justified by DynaMAGNA++'s superiority over MAGNA++ in terms of alignment quality.

DynaMAGNA++'s availability. We implement a friendly graphical user interface (GUI) for DynaMAGNA++ (Fig. 7) for

Table 4. Alignment quality of DynaMAGNA++ optimizing both dynamic edge and node conservation (E + N), dynamic edge conservation alone (E), and dynamic node conservation alone (N), in terms of node correctness, when each network is aligned to itself (corresponding to the 0% noise level)

NA method \ Network	Zebra	Yeast	Enron
DynaMAGNA++ (E+N)	**0.800**	**0.920**	**1.000**
DynaMAGNA++ (E)	0.704	0.635	**1.000**
DynaMAGNA++ (N)	0.793	0.891	0.996

Note: Each score is an average over five runs. In each column, the highest score is bolded.
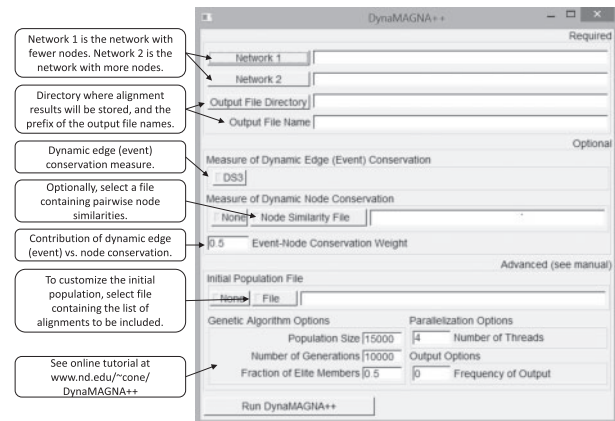

Fig. 7. GUI to DynaMAGNA++. The only required parameters are the two networks to be aligned, and the output directory/file name information. While DS[3] is the only currently implemented dynamic edge (event) conservation measure, other future dynamic edge conservation measures can be easily added. Any dynamic node similarity measure can be used by selecting a file containing pairwise similarities between nodes of the two networks. The α parameter (Section 2.2) can be set to any desired value. Other advanced parameters can also be user-specified. The default values are set according to the parameter values used in this work (Section 2.2)

easy use by domain (e.g., biological) scientists. Also, we provide the source code of DynaMAGNA++ so that computational scientists may potentially extend the work (http://nd.edu/~cone/ DynaMAGNA++/).

4 Conclusion

We introduce the first ever dynamic NA method. We show that our method, DynaMAGNA++, produces superior alignments compared to its static NA counterpart due to its explicit use of available temporal information in dynamic network data. DynaMAGNA++ is a search-based NA method that can optimize any alignment quality measure. In this work, we propose an efficient temporal information-based alignment quality measure, DS[3], that DynaMAGNA++ partly optimizes in order to find good alignments. DynaMAGNA++ can be extended in two ways: by optimizing future, potentially more efficient alignment quality measures with the current search strategy, or by optimizing its current alignment quality measures with a future, potentially superior search strategy (Crawford *et al.*, 2015). DynaMAGNA++ can also be extended into an "online" version to allow for dealing with constantly "arriving" temporal data (Albers, 2003). Namely, after DynaMAGNA++ has produced an alignment of two dynamic

networks, if new events are added to either of the networks, DynaMAGNA++ can be modified to allow for updating the current alignment into a new one that will account for the new events.

We demonstrate applicability of DynaMAGNA++ and dynamic NA in general in multiple domains: biological networks (ecological networks and PINs) and social networks. Given the impact that static NA has had in computational biology, as more PIN and other molecular dynamic network data are becoming available, dynamic NA and thus our study will continue to gain importance. The same holds for other domains in which increasing amounts of real-world dynamic network data are being collected. So, we have just scratched the tip of the iceberg called dynamic NA.

Funding

Conflict of Interest: none declared.

References

Albers,S. (2003) Online algorithms: a survey. *Math. Program.*, 97, 3–26.

Bayati,M. *et al.* (2013) Message-passing algorithms for sparse network alignment. *ACM Trans. Knowl. Discov. Data*, 73, 1–3. 31.

Boccaletti, S. *et al.* (2006) Complex networks: structure and dynamics. *Phys. Rep.*, 424, 175–308.

Crawford, J. *et al.* (2015) Fair evaluation of global network aligners. *Algorith. Mol. Biol.*, 10.

Duchenne,O. *et al.* (2011) A tensor-based algorithm for high-order graph matching. *Pattern Anal. Machine Intel., IEEE Trans.*, 33, 2383–2395.

Elmsallati,A. *et al.* (2016) Global alignment of protein-protein interaction networks: a survey. *IEEE/ACM Trans. Comput. Biol. Bioinform.*, 13, 689–705.

Emmert-Streib,F. *et al.* (2016) Fifty years of graph matching, network alignment and network comparison. *Info. Sci.*, 346 (C,), 180–197.

Faisal,F. *et al.* (2015a) Global network alignment in the context of aging. *IEEE/ACM Trans. Comput. Biol. Bioinform.*, 12, 40–52.

Faisal,F. *et al.* (2015b) The post-genomic era of biological network alignment. *EURASIP J. Bioinform. Systems Biol.*, 2015, 1–19.

Guzzi,P.H. and Milenković,T. (2017) Survey of local and global biological network alignment: the need to reconcile the two sides of the same coin. *Brief. Bioinform.*, doi: 10.1093/bib/bbw132.

Holme,P. (2015) Modern temporal network theory: a colloquium. *Eur. Phys. J. B*, 88, 1–30.

Hočevar,T. and Demšar,J. (2014) A combinatorial approach to graphlet counting. *Bioinformatics*, 30, 559–565.

Hulovatyy,Y. *et al.* (2014) Revealing missing parts of the interactome via link prediction. *PLOS One*, 9, e90073.

Hulovatyy,Y. *et al.* (2015) Exploring the structure and function of temporal networks with dynamic graphlets. *Bioinformatics*, 31, 171–180.

Ibragimov,R. *et al.* (2013). GEDEVO: an evolutionary graph edit distance algorithm for biological network alignment. In *GCB*, pages 68–79.

Kuchaiev,O. and Pržulj,N. (2011) Integrative network alignment reveals large regions of global network similarity in yeast and human. *Bioinformatics*, 27, 1390–1396.

Kuchaiev,O. *et al.* (2010) Topological network alignment uncovers biological function and phylogeny. *J. R Soc. Interf.*, 7, 1341–1354.

Mamano,N. and Hayes,W.B. (2017) SANA: simulated annealing far outperforms many other search algorithms for biological network alignment. *Bioinformatics*, doi: 10.1093/bioinformatics/btx090.

Malod-Dognin,N. and Pržulj,N. (2015) L-GRAAL: Lagrangian graphlet-based network aligner. *Bioinformatics*, 31, 2182–2189.

Meng,L. *et al.* (2016a). IGLOO: integrating global and local biological network alignment. In *Proc. of Workshop on Mining and Learning with Graphs (MLG) at the Conference on Knowledge Discovery and Data Mining (KDD)*.

Meng,L. *et al.* (2016b) Local versus global biological network alignment. *Bioinformatics*, 32, 3155–3164.

Milenković,T. and Pržulj,N. (2008) Uncovering biological network function via graphlet degree signatures. *Cancer Inform.*, 6, 257–273.

Milenković,T. *et al.* (2010) Optimal network alignment with graphlet degree vectors. *Cancer Inform.*, 9, 121–137.

Neyshabur,B. *et al.* (2013) NETAL: a new graph-based method for global alignment of protein-protein interaction networks. *Bioinformatics*, 29, 1654–1662.

Patro,R. and Kingsford,C. (2012) Global network alignment using multiscale spectral signatures. *Bioinformatics*, 28, 3105–3114.

Priebe,C.E. *et al.* (2005) Scan statistics on Enron graphs. *Comput. Math. Organ. Theory*, 11, 229–247.

Pržulj,N. *et al.* (2010). Geometric evolutionary dynamics of protein interaction networks. In *Proc. of the Pacific Symposium Biocomputing*, pages 4–8.

Przytycka,T.M. and Kim,Y.-A. (2010) Network integration meets network dynamics. *BMC Bioinform.*, 8.

Przytycka,T.M. *et al.* (2010) Toward the dynamic interactome: it's about time. *Brief. Bioinform.*, 11, 15–29.

Rubenstein,D.I. *et al.* (2015) Similar but different: dynamic social network analysis highlights fundamental differences between the fission-fusion societies of two equid species, the onager and Grevy's zebra. *PLOS One*, 10, e0138645.

Saraph,V. and Milenković,T. (2014) MAGNA: Maximizing Accuracy in Global Network Alignment. *Bioinformatics*, 30, 2931–2940.

Singh,R. *et al.* (2007). Pairwise global alignment of protein interaction networks by matching neighborhood topology. In: *Research in Computational Molecular Biology*. Springer, Oakland, CA, USA, pp. 16–31.

Sun,Y. *et al.* (2015). Simultaneous optimization of both node and edge conservation in network alignment via WAVE. In *Proc. of Workshop on Algorithms in Bioinformatics (WABI)*, Atlanta, GA, USA, pp. 16–39.

Vijayan,V. and Milenković,T. (2016). Multiple network alignment via multiMAGNA++. In *Proc. of Workshop on Data Mining in Bioinformatics (BIOKDD) at the Conference on Knowledge Discovery and Data Mining* (KDD).

Vijayan,V. *et al.* (2015) MAGNA++: Maximizing Accuracy in Global Network Alignment via both node and edge conservation. *Bioinformatics*, 31, 2409–2411.

Yaveroğlu,Ö. *et al.* (2015) Proper evaluation of alignment-free network comparison methods. *Bioinformatics*, 31, 2697–2704.

Zhang,Y. *et al.* (2015). COSNET: connecting heterogeneous social networks with local and global consistency. In *Proc. ACM SIGKDD Int. Conf. on Knowledge Discovery and Data Mining*, pages 1485–1494.